crystals

MDPI

Editorial

Serial X-ray Crystallography

Ki Hyun Nam [1,2]

[1] Department of Life Science, Pohang University of Science and Technology, Pohang 37673, Korea; structures@postech.ac.kr
[2] POSTECH Biotech Center, Pohang University of Science and Technology, Pohang 37673, Korea

Abstract: Serial crystallography (SX) is an emerging technique to determine macromolecules at room temperature. SX with a pump–probe experiment provides the time-resolved dynamics of target molecules. SX has developed rapidly over the past decade as a technique that not only provides room-temperature structures with biomolecules, but also has the ability to time-resolve their molecular dynamics. The serial femtosecond crystallography (SFX) technique using an X-ray free electron laser (XFEL) has now been extended to serial synchrotron crystallography (SSX) using synchrotron X-rays. The development of a variety of sample delivery techniques and data processing programs is currently accelerating SX research, thereby increasing the research scope. In this editorial, I briefly review some of the experimental techniques that have contributed to advances in the field of SX research and recent major research achievements. This Special Issue will contribute to the field of SX research.

Keywords: serial crystallography; serial femtosecond crystallography; serial synchrotron crystallography; room temperature; radiation damage; time-resolved; pump–probe

Citation: Nam, K.H. Serial X-ray Crystallography. *Crystals* **2022**, *12*, 99. https://doi.org/10.3390/cryst12010099

Academic Editor: Abel Moreno

Received: 1 January 2022
Accepted: 5 January 2022
Published: 13 January 2022

Traditional X-ray crystallography using single crystals has contributed to scientific developments, not only in the field of biological research, but also in the medical industry, and has shown rapid growth over the past few decades [1,2]. This method is still considered a powerful structural biology technique and is still familiar to many structural biologist. However, long-term exposure of X-rays to single crystals during data collection causes radiation damage by *K*-shell photoionization and Auger decay, which significantly reduces the quality of diffraction data and permits irreversible structural changes [3,4]. Radiation damage can be reduced through general application of data collection at cryogenic temperatures [5–7], but it does not completely annul radiation damage, and cryogenic structural information may be limited in terms of molecular dynamics [8]. If these experimental limitations can be addressed, we will be able to better understand biomolecules and utilize them for applications.

SX crystallography can significantly overcome the experimental limitations of traditional X-ray crystallography [9–11]. In SX, radiation damage can be minimized because intense XFEL or synchrotron X-rays are used to collect data by exposing the crystals to X-rays for a very short time and only once [4,12–15]. Additionally, it is useful for understanding the function of molecules in terms of molecular dynamics because data collection is possible at room temperature or at near-physiological temperature [16,17]. Furthermore, by capturing structural changes at critical points in molecular activity through pump–probe experiments, it is possible to accurately distinguish molecular reaction mechanisms [18,19].

The serial femtosecond crystallography (SFX) research field has contributed to many technological and scientific developments over the past decade [10]. However, due to the limited beamtime of XFEL, there has been a limit to the magnification at the user base [20]. However, in recent years, this has been extended to serial synchrotron crystallography (SSX) due to the development of a detector capable of fast readouts along with a technique for focusing X-rays at high photon flux in a synchrotron [20] (Figure 1).

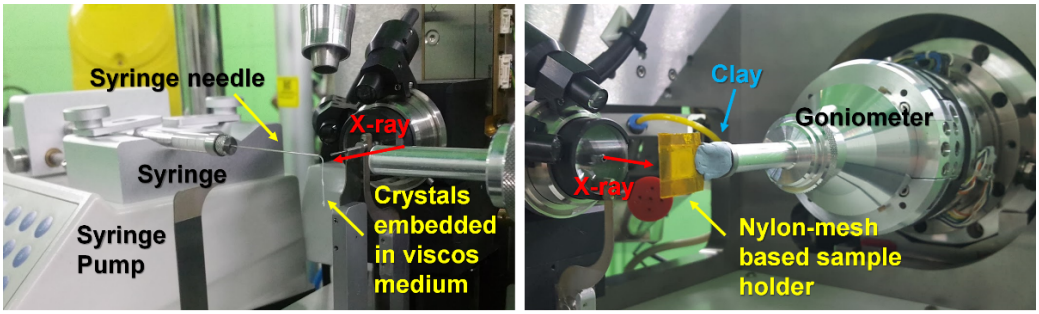

Figure 1. Photo of the experimental setup of serial synchrotron crystallography (SSX). (**left**) Delivery of crystals embedding viscous medium via a syringe and syringe pump [21]. (**right**) Fixed-target scanning using nylon-mesh and enclosing film (NAM) holder [22].

There are certainly differences in the studies that can be performed because the peak brightness and time jitter provided by XFEL and synchrotron X-ray are different, but both techniques can provide structural information that is more biologically relevant compared to conventional X-ray crystallography. However, in the SX experiment, since X-rays are only exposed to the crystal sample once, a large number of crystals are required, along with a technique for continuously delivering the crystals to the X-ray location [23]. These aspects imply that SX is experimentally challenging when compared with traditional X-ray crystallography.

In terms of the sample delivery, the gas dynamic virtual nozzle (GDVN)-based liquid jet injector [24] has been usefully applied at the XFEL facility with a high repetition rate since the early days of SX. Injectors that have been recently developed are evolving to enable time-resolved studies by internally mixing substrates or inhibitors with protein crystals [25–27]. Additionally, after the development of lipid cubic phase (LCP) injectors [28,29], which could reduce sample consumption at the XFEL facility with a low repetition rate or synchrotron, various viscous materials, such as different types of grease [30–33], Vaseline [34], agarose [35], hyaluronic acid [32], hydroxyethyl cellulose [31], carboxymethyl cellulose sodium salt [36], pluronic F-127 [36], polyethylene oxide [37], polyacrylamide [38], wheat starch [39], alginate [39], shortening [40], and lard [41], were developed and applied. This provided an opportunity to deliver samples according to the characteristics of crystal samples [23]. Another notable sample delivery system is the fixed-target scanning method, which consists of less crystal consumption and less physical stress to crystal samples when compared with injection methods. Currently, various types of fixed-target sample holders have been developed using silicon nitride [42,43], graphene [44], mesh [22,45–47], and viscous medium [48] to stably fix crystals to the sample holder. Additionally, other sample delivery methods, such as microfluidics [49–51], capillaries [52,53], and conveyer belts [54], have been developed. Moreover, recently the "hit-and-return" (HARE) [55] and drop-on-drop methods [56] were developed for time-resolved SX experiments and molecular movies have been successfully visualized. Although there are differences depending on the sample delivery device obtained by the facility or beamline, a pool of sample delivery systems that researchers can select from according to the characteristics of the crystal sample is provided. During the SX experiment, the crystals cannot provide a perfectly continuous X-ray position. Accordingly, the collected images include diffraction-free, single-crystal diffraction, and multiple crystal diffraction patterns. In early SX studies, multi-crystal diffraction patterns were considered to inhibit the indexing of Bragg peaks, but with the development of serial crystallography programs, it has been developed to extract multiple diffraction patterns from one image [57,58].

Using the SX technique, various room- or nearly physiological-temperature structures have been determined [16,17,59–61]. This will provide useful information for understanding the flexibility of molecules when compared with cryogenic structures. Moreover, the time-resolved SX technique enables the visualization of the precision molecular change using the pump–probe experiment [18]. Time-resolved SX studies using optical lasers

are already routinely performed at the SX experimental hutch and elucidate molecular structures. Recently, photoactive states of rhodopsin [62], bacteriorhodopsin [63], photosystem II [64,65], phytochrome BphP [66], fluorescent protein [67], and photoactive yellow protein [68] have been analyzed using an optical pump. These results elucidate a more detailed mechanism of the structural change of the molecule, together with spectroscopic results. Meanwhile, in nature, many enzymes experience a reaction of cleavage, attachment, or modification of a target substrate. Consequently, it is very important to understand the molecular action to time-resolve the structural change by adding a substrate or inhibitor to the crystal sample. Recently, time-resolution studies for hydratase [69], cytochrome c oxidase [70], and β-lactamase [71] using a solution pump application have been reported. These remarkable advances in time-resolved SX research could be used as a very useful tool to further understand life phenomena. In the future, more SX studies will enable a more robust analysis of molecular functions.

This Special Issue is intended to cover a broad range of topics related to SX research. This includes general SX data structure analysis, as well as experimental technique development and new SX research approaches. Additionally, we would like to cover a wide range of topics, such as negative experimental results of SX and X-ray crystallography techniques, which could potentially contribute to SX research. Therefore, we believe that this Special Issue will make an academic contribution to the field of SX research.

Funding: This research was funded by the National Research Foundation of Korea (NRF-2017M3A9F 6029736, NRF-2020M3H1A1075314 and NRF-2021R1I1A1A01050838).

Institutional Review Board Statement: Not applicable.

Informed Consent Statement: Not applicable.

Conflicts of Interest: The author declares no conflict of interest.

References

1. Pomés, A.; Chruszcz, M.; Gustchina, A.; Minor, W.; Mueller, G.A.; Pedersen, L.C.; Wlodawer, A.; Chapman, M.D. 100 Years later: Celebrating the contributions of x-ray crystallography to allergy and clinical immunology. *J. Allergy Clin. Immunol.* **2015**, *136*, 29–37.e10. [CrossRef]
2. Blundell, T.L. Protein crystallography and drug discovery: Recollections of knowledge exchange between academia and industry. *IUCrJ* **2017**, *4*, 308–321. [CrossRef] [PubMed]
3. Lomb, L.; Barends, T.R.M.; Kassemeyer, S.; Aquila, A.; Epp, S.; Erk, B.; Foucar, L.; Hartmann, R.; Rudek, B.; Rolles, D.; et al. Radiation damage in protein serial femtosecond crystallography using an x-ray free-electron laser. *Phys. Rev. B* **2011**, *84*, 214111. [CrossRef]
4. Chapman, H.N.; Fromme, P.; Barty, A.; White, T.A.; Kirian, R.A.; Aquila, A.; Hunter, M.S.; Schulz, J.; DePonte, D.P.; Weierstall, U.; et al. Femtosecond X-ray protein nanocrystallography. *Nature* **2011**, *470*, 73–77. [CrossRef] [PubMed]
5. Rodgers, D.W. Cryocrystallography. *Structure* **1994**, *2*, 1135–1140. [CrossRef]
6. Watenpaugh, K.D. Macromolecular crystallography at cryogenic temperatures: Current Opinion in Structural Biology 1991, 1: 1012–1015. *Curr. Opin. Struct. Biol.* **1991**, *1*, 1012–1015. [CrossRef]
7. Meents, A.; Gutmann, S.; Wagner, A.; Schulze-Briese, C. Origin and temperature dependence of radiation damage in biological samples at cryogenic temperatures. *Proc. Natl. Acad. Sci. USA* **2009**, *107*, 1094–1099. [CrossRef]
8. Nam, K. Molecular Dynamics—From Small Molecules to Macromolecules. *Int. J. Mol. Sci.* **2021**, *22*, 3761. [CrossRef]
9. Boutet, S.; Lomb, L.; Williams, G.J.; Barends, T.R.M.; Aquila, A.; Doak, R.B.; Weierstall, U.; DePonte, D.P.; Steinbrener, J.; Shoeman, R.L.; et al. High-Resolution Protein Structure Determination by Serial Femtosecond Crystallography. *Science* **2012**, *337*, 362–364. [CrossRef]
10. Martin-Garcia, J. Protein Dynamics and Time Resolved Protein Crystallography at Synchrotron Radiation Sources: Past, Present and Future. *Crystals* **2021**, *11*, 521. [CrossRef]
11. Nam, K.-H. Approach of Serial Crystallography II. *Crystals* **2021**, *11*, 655. [CrossRef]
12. Fromme, P.; Spence, J.C. Femtosecond nanocrystallography using X-ray lasers for membrane protein structure determination. *Curr. Opin. Struct. Biol.* **2011**, *21*, 509–516. [CrossRef]
13. Schlichting, I. Serial femtosecond crystallography: The first five years. *IUCrJ* **2015**, *2*, 246–255. [CrossRef]
14. Martin-Garcia, J.M.; Conrad, C.E.; Coe, J.; Roy-Chowdhury, S.; Fromme, P. Serial femtosecond crystallography: A revolution in structural biology. *Arch. Biochem. Biophys.* **2016**, *602*, 32–47. [CrossRef]
15. Kim, J.; Kim, H.-Y.; Park, J.; Kim, S.; Kim, S.; Rah, S.; Lim, J.; Nam, K.H. Focusing X-ray free-electron laser pulses using Kirkpatrick–Baez mirrors at the NCI hutch of the PAL-XFEL. *J. Synchrotron Radiat.* **2018**, *25*, 289–292. [CrossRef]

16. Durdagi, S.; Dağ, J.; Dogan, B.; Yigin, M.; Avsar, T.; Buyukdag, C.; Erol, I.; Ertem, F.B.; Calis, S.; Yildirim, G.; et al. Near-physiological-temperature serial crystallography reveals conformations of SARS-CoV-2 main protease active site for improved drug repurposing. *Structure* **2021**, *29*, 1382–1396.e1386. [CrossRef]
17. Nam, K. Room-Temperature Structure of Xylitol-Bound Glucose Isomerase by Serial Crystallography: Xylitol Binding in the M1 Site Induces Release of Metal Bound in the M2 Site. *Int. J. Mol. Sci.* **2021**, *22*, 3892. [CrossRef] [PubMed]
18. Brändén, G.; Neutze, R. Advances and challenges in time-resolved macromolecular crystallography. *Science* **2021**, *373*, eaba0954. [CrossRef]
19. Schmidt, M. Time-Resolved Macromolecular Crystallography at Pulsed X-ray Sources. *Int. J. Mol. Sci.* **2019**, *20*, 1401. [CrossRef] [PubMed]
20. Nam, K.H. Approach of Serial Crystallography. *Crystals* **2020**, *10*, 854. [CrossRef]
21. Park, S.-Y.; Nam, K.H. Sample delivery using viscous media, a syringe and a syringe pump for serial crystallography. *J. Synchrotron Radiat.* **2019**, *26*, 1815–1819. [CrossRef] [PubMed]
22. Park, S.-Y.; Choi, H.; Eo, C.; Cho, Y.; Nam, K.H. Fixed-Target Serial Synchrotron Crystallography Using Nylon Mesh and Enclosed Film-Based Sample Holder. *Crystals* **2020**, *10*, 803. [CrossRef]
23. Nam, K.H. Sample Delivery Media for Serial Crystallography. *Int. J. Mol. Sci.* **2019**, *20*, 1094. [CrossRef] [PubMed]
24. DePonte, D.P.; Weierstall, U.; Schmidt, K.; Warner, J.; Starodub, D.; Spence, J.C.H.; Doak, R.B. Gas dynamic virtual nozzle for generation of microscopic droplet streams. *J. Phys. D Appl. Phys.* **2008**, *41*, 195505. [CrossRef]
25. Calvey, G.D.; Katz, A.M.; Pollack, L. Microfluidic Mixing Injector Holder Enables Routine Structural Enzymology Measurements with Mix-and-Inject Serial Crystallography Using X-ray Free Electron Lasers. *Anal. Chem.* **2019**, *91*, 7139–7144. [CrossRef] [PubMed]
26. Calvey, G.D.; Katz, A.M.; Schaffer, C.B.; Pollack, L. Mixing injector enables time-resolved crystallography with high hit rate at X-ray free electron lasers. *Struct. Dyn.* **2016**, *3*, 054301. [CrossRef] [PubMed]
27. Knoška, J.; Adriano, L.; Awel, S.; Beyerlein, K.R.; Yefanov, O.; Oberthuer, D.; Murillo, G.E.P.; Roth, N.; Sarrou, I.; Villanueva-Perez, P.; et al. Ultracompact 3D microfluidics for time-resolved structural biology. *Nat. Commun.* **2020**, *11*, 657. [CrossRef] [PubMed]
28. Weierstall, U.; James, D.; Wang, C.; White, T.A.; Wang, D.; Liu, W.; Spence, J.C.H.; Doak, R.B.; Nelson, G.; Fromme, P.; et al. Lipidic cubic phase injector facilitates membrane protein serial femtosecond crystallography. *Nat. Commun.* **2014**, *5*, 3309. [CrossRef]
29. Liu, W.; Ishchenko, A.; Cherezov, V. Preparation of microcrystals in lipidic cubic phase for serial femtosecond crystallography. *Nat. Protoc.* **2014**, *9*, 2123–2134. [CrossRef]
30. Sugahara, M.; Mizohata, E.; Nango, E.; Suzuki, M.; Tanaka, T.; Masuda, T.; Tanaka, R.; Shimamura, T.; Tanaka, Y.; Suno, C.; et al. Grease matrix as a versatile carrier of proteins for serial crystallography. *Nat. Methods* **2014**, *12*, 61–63. [CrossRef]
31. Sugahara, M.; Nakane, T.; Masuda, T.; Suzuki, M.; Inoue, S.; Song, C.; Tanaka, R.; Nakatsu, T.; Mizohata, E.; Yumoto, F.; et al. Hydroxyethyl cellulose matrix applied to serial crystallography. *Sci. Rep.* **2017**, *7*, 703. [CrossRef]
32. Sugahara, M.; Song, C.; Suzuki, M.; Masuda, T.; Inoue, S.; Nakane, T.; Yumoto, F.; Nango, E.; Tanaka, R.; Tono, K.; et al. Oil-free hyaluronic acid matrix for serial femtosecond crystallography. *Sci. Rep.* **2016**, *6*, 24484. [CrossRef]
33. Sugahara, M.; Motomura, K.; Suzuki, M.; Masuda, T.; Joti, Y.; Numata, K.; Tono, K.; Yabashi, M.; Ishikawa, T. Viscosity-adjustable grease matrices for serial nanocrystallography. *Sci. Rep.* **2020**, *10*, 1371. [CrossRef]
34. Botha, S.; Nass, K.; Barends, T.R.M.; Kabsch, W.; Latz, B.; Dworkowski, F.; Foucar, L.; Panepucci, E.; Wang, M.; Shoeman, R.L.; et al. Room-temperature serial crystallography at synchrotron X-ray sources using slowly flowing free-standing high-viscosity microstreams. *Acta Crystallogr. Sect. D Biol. Crystallogr.* **2015**, *71*, 387–397. [CrossRef]
35. Conrad, C.E.; Basu, S.; James, D.; Wang, D.; Schaffer, A.; Roy-Chowdhury, S.; Zatsepin, N.; Aquila, A.; Coe, J.; Gati, C.; et al. A novel inert crystal delivery medium for serial femtosecond crystallography. *IUCrJ* **2015**, *2*, 421–430. [CrossRef]
36. Kovácsová, G.; Grünbein, M.L.; Kloos, M.; Barends, T.R.M.; Schlesinger, R.; Heberle, J.; Kabsch, W.; Shoeman, R.L.; Doak, R.B.; Schlichting, I. Viscous hydrophilic injection matrices for serial crystallography. *IUCrJ* **2017**, *4*, 400–410. [CrossRef]
37. Martin-Garcia, J.M.; Conrad, C.E.; Nelson, G.; Stander, N.; Zatsepin, N.A.; Zook, J.; Zhu, L.; Geiger, J.; Chun, E.; Kissick, D.; et al. Serial millisecond crystallography of membrane and soluble protein microcrystals using synchrotron radiation. *IUCrJ* **2017**, *4*, 439–454. [CrossRef]
38. Park, J.; Park, S.; Kim, J.; Park, G.; Cho, Y.; Nam, K.H. Polyacrylamide injection matrix for serial femtosecond crystallography. *Sci. Rep.* **2019**, *9*, 1–8. [CrossRef] [PubMed]
39. Nam, K.H. Polysaccharide-Based Injection Matrix for Serial Crystallography. *Int. J. Mol. Sci.* **2020**, *21*, 3332. [CrossRef] [PubMed]
40. Nam, K.H. Shortening injection matrix for serial crystallography. *Sci. Rep.* **2020**, *10*, 1–8. [CrossRef] [PubMed]
41. Nam, K.H. Lard Injection Matrix for Serial Crystallography. *Int. J. Mol. Sci.* **2020**, *21*, 5977. [CrossRef]
42. Hunter, M.S.; Segelke, B.; Messerschmidt, M.; Williams, G.J.; Zatsepin, N.; Barty, A.; Benner, W.H.; Carlson, D.B.; Coleman, M.; Graf, A.; et al. Fixed-target protein serial microcrystallography with an x-ray free electron laser. *Sci. Rep.* **2014**, *4*, srep06026. [CrossRef] [PubMed]
43. Murray, T.D.; Lyubimov, A.Y.; Ogata, C.M.; Vo, H.; Uervirojnangkoorn, M.; Brunger, A.T.; Berger, J.M. A high-transparency, micro-patternable chip for X-ray diffraction analysis of microcrystals under native growth conditions. *Acta Crystallogr. Sect. D Biol. Crystallogr.* **2015**, *71*, 1987–1997. [CrossRef] [PubMed]
44. Sui, S.; Wang, Y.; Kolewe, K.W.; Srajer, V.; Henning, R.; Schiffman, J.D.; Dimitrakopoulos, C.; Perry, S.L. Graphene-based microfluidics for serial crystallography. *Lab Chip* **2016**, *16*, 3082–3096. [CrossRef] [PubMed]

45. Lee, D.; Baek, S.; Park, J.; Lee, K.; Kim, J.; Lee, S.J.; Chung, W.K.; Lee, J.-L.; Cho, Y.; Nam, K.H. Nylon mesh-based sample holder for fixed-target serial femtosecond crystallography. *Sci. Rep.* **2019**, *9*, 6971. [CrossRef] [PubMed]
46. Nam, K.H.; Kim, J.; Cho, Y. Polyimide mesh-based sample holder with irregular crystal mounting holes for fixed-target serial crystallography. *Sci. Rep.* **2021**, *11*, 13115. [CrossRef]
47. Owen, R.; Nanao, M.; Pearson, A.R. Multi and serial data collection and processing. *Acta Crystallogr. Sect. D Struct. Biol.* **2019**, *75*, 111–112. [CrossRef]
48. Lee, K.; Lee, D.; Baek, S.; Park, J.; Lee, S.J.; Park, S.; Chung, W.K.; Lee, J.-L.; Cho, H.-S.; Cho, Y.; et al. Viscous-medium-based crystal support in a sample holder for fixed-target serial femtosecond crystallography. *J. Appl. Crystallogr.* **2020**, *53*, 1051–1059. [CrossRef]
49. Monteiro, D.C.F.; Vakili, M.; Harich, J.; Sztucki, M.; Meier, S.M.; Horrell, S.; Josts, I.; Trebbin, M. A microfluidic flow-focusing device for low sample consumption serial synchrotron crystallography experiments in liquid flow. *J. Synchrotron Radiat.* **2019**, *26*, 406–412. [CrossRef]
50. Monteiro, D.C.F.; Von Stetten, D.; Stohrer, C.; Sans, M.; Pearson, A.R.; Santoni, G.; Van Der Linden, P.; Trebbin, M. 3D-MiXD: 3D-printed X-ray-compatible microfluidic devices for rapid, low-consumption serial synchrotron crystallography data collection in flow. *IUCrJ* **2020**, *7*, 207–219. [CrossRef]
51. Nam, K.H.; Cho, Y. Stable sample delivery in a viscous medium via a polyimide-based single-channel microfluidic chip for serial crystallography. *J. Appl. Crystallogr.* **2021**, *54*, 1081–1087. [CrossRef]
52. Stellato, F.; Oberthür, D.; Liang, M.; Bean, R.; Gati, C.; Yefanov, O.; Barty, A.; Burkhardt, A.; Fischer, P.; Galli, L.; et al. Room-temperature macromolecular serial crystallography using synchrotron radiation. *IUCrJ* **2014**, *1*, 204–212. [CrossRef] [PubMed]
53. Nam, K.H. Stable sample delivery in viscous media via a capillary for serial crystallography. *J. Appl. Crystallogr.* **2020**, *53*, 45–50. [CrossRef]
54. Beyerlein, K.R.; Dierksmeyer, D.; Mariani, V.; Kuhn, M.; Sarrou, I.; Ottaviano, A.; Awel, S.; Knoska, J.; Fuglerud, S.; Jönsson, O.; et al. Mix-and-diffuse serial synchrotron crystallography. *IUCrJ* **2017**, *4*, 769–777. [CrossRef] [PubMed]
55. Schulz, E.C.; Mehrabi, P.; Mueller-Werkmeister, H.; Tellkamp, F.; Jha, A.; Stuart, W.; Persch, E.; De Gasparo, R.; Diederich, F.; Pai, E.F.; et al. The hit-and-return system enables efficient time-resolved serial synchrotron crystallography. *Nat. Methods* **2018**, *15*, 901–904. [CrossRef] [PubMed]
56. Butryn, A.; Simon, P.S.; Aller, P.; Hinchliffe, P.; Massad, R.N.; Leen, G.; Tooke, C.L.; Bogacz, I.; Kim, I.-S.; Bhowmick, A.; et al. An on-demand, drop-on-drop method for studying enzyme catalysis by serial crystallography. *Nat. Commun.* **2021**, *12*, 4461. [CrossRef]
57. White, T.A.; Mariani, V.; Brehm, W.; Yefanov, O.; Barty, A.; Beyerlein, K.R.; Chervinskii, F.; Galli, L.; Gati, C.; Nakane, T.; et al. Recent developments in CrystFEL. *J. Appl. Crystallogr.* **2016**, *49*, 680–689. [CrossRef]
58. White, T.A. Processing serial crystallography data with CrystFEL: A step-by-step guide. *Acta Crystallogr. Sect. D Struct. Biol.* **2019**, *75*, 219–233. [CrossRef]
59. Cellini, A.; Wahlgren, W.Y.; Henry, L.; Pandey, S.; Ghosh, S.; Castillon, L.; Claesson, E.; Takala, H.; Kübel, J.; Nimmrich, A.; et al. The three-dimensional structure of Drosophila melanogaster (6–4) photolyase at room temperature. *Acta Crystallogr. Sect. D Struct. Biol.* **2021**, *77*, 1001–1009. [CrossRef]
60. Liu, H.; Deepak, R.N.V.K.; Shiriaeva, A.; Gati, C.; Batyuk, A.; Hu, H.; Weierstall, U.; Liu, W.; Wang, L.; Cherezov, V.; et al. Molecular basis for lipid recognition by the prostaglandin D_2 receptor CRTH2. *Proc. Natl. Acad. Sci. USA* **2021**, *118*, e2102813118. [CrossRef]
61. Wilamowski, M.; Sherrell, D.A.; Minasov, G.; Kim, Y.; Shuvalova, L.; Lavens, A.; Chard, R.; Maltseva, N.; Jedrzejczak, R.; Rosas-Lemus, M.; et al. 2′-O methylation of RNA cap in SARS-CoV-2 captured by serial crystallography. *Proc. Natl. Acad. Sci. USA* **2021**, *118*, e2100170118. [CrossRef] [PubMed]
62. Skopintsev, P.; Ehrenberg, D.; Weinert, T.; James, D.; Kar, R.K.; Johnson, P.J.M.; Ozerov, D.; Furrer, A.; Martiel, I.; Dworkowski, F.; et al. Femtosecond-to-millisecond structural changes in a light-driven sodium pump. *Nature* **2020**, *583*, 314–318. [CrossRef] [PubMed]
63. Kovacs, G.N.; Colletier, J.-P.; Grünbein, M.L.; Yang, Y.; Stensitzki, T.; Batyuk, A.; Carbajo, S.; Doak, R.B.; Ehrenberg, D.; Foucar, L.; et al. Three-dimensional view of ultrafast dynamics in photoexcited bacteriorhodopsin. *Nat. Commun.* **2019**, *10*, 3177. [CrossRef] [PubMed]
64. Ibrahim, M.; Fransson, T.; Chatterjee, R.; Cheah, M.H.; Hussein, R.; Lassalle, L.; Sutherlin, K.D.; Young, I.D.; Fuller, F.D.; Gul, S.; et al. Untangling the sequence of events during the S2 → S3transition in photosystem II and implications for the water oxidation mechanism. *Proc. Natl. Acad. Sci. USA* **2020**, *117*, 12624–12635. [CrossRef]
65. Suga, M.; Akita, F.; Yamashita, K.; Nakajima, Y.; Ueno, G.; Li, H.; Yamane, T.; Hirata, K.; Umena, Y.; Yonekura, S.; et al. An oxyl/oxo mechanism for oxygen-oxygen coupling in PSII revealed by an x-ray free-electron laser. *Science* **2019**, *366*, 334–338. [CrossRef]
66. Claesson, E.; Wahlgren, W.Y.; Takala, H.; Pandey, S.; Castillon, L.; Kuznetsova, V.; Henry, L.; Panman, M.; Carrillo, M.; Kübel, J.; et al. The primary structural photoresponse of phytochrome proteins captured by a femtosecond X-ray laser. *eLife* **2020**, *9*, e53514. [CrossRef]

67. Woodhouse, J.; Kovacs, G.N.; Coquelle, N.; Uriarte, L.M.; Adam, V.; Barends, T.R.M.; Byrdin, M.; De La Mora, E.; Doak, R.B.; Feliks, M.; et al. Photoswitching mechanism of a fluorescent protein revealed by time-resolved crystallography and transient absorption spectroscopy. *Nat. Commun.* **2020**, *11*, 741. [CrossRef]
68. Pandey, S.; Bean, R.; Sato, T.; Poudyal, I.; Bielecki, J.; Villarreal, J.C.; Yefanov, O.; Mariani, V.; White, T.A.; Kupitz, C.; et al. Time-resolved serial femtosecond crystallography at the European XFEL. *Nat. Methods* **2019**, *17*, 73–78. [CrossRef]
69. Dasgupta, M.; Budday, D.; de Oliveira, S.H.P.; Madzelan, P.; Marchany-Rivera, D.; Seravalli, J.; Hayes, B.; Sierra, R.G.; Boutet, S.; Hunter, M.S.; et al. Mix-and-inject XFEL crystallography reveals gated conformational dynamics during enzyme catalysis. *Proc. Natl. Acad. Sci. USA* **2019**, *116*, 25634–25640. [CrossRef]
70. Ishigami, I.; Lewis-Ballester, A.; Echelmeier, A.; Brehm, G.; Zatsepin, N.A.; Grant, T.D.; Coe, J.D.; Lisova, S.; Nelson, G.; Zhang, S.; et al. Snapshot of an oxygen intermediate in the catalytic reaction of cytochrome c oxidase. *Proc. Natl. Acad. Sci. USA* **2019**, *116*, 3572–3577. [CrossRef]
71. Pandey, S.; Calvey, G.; Katz, A.M.; Malla, T.N.; Koua, F.H.M.; Martin-Garcia, J.M.; Poudyal, I.; Yang, J.-H.; Vakili, M.; Yefanov, O.; et al. Observation of substrate diffusion and ligand binding in enzyme crystals using high-repetition-rate mix-and-inject serial crystallography. *IUCrJ* **2021**, *8*, 878–895. [CrossRef] [PubMed]